CrossMark

Photochemical production of polyols arising from significant photo-transformation of dissolved organic matter in the oligotrophic surface ocean

Michael Gonsior [a,b,*], Norbert Hertkorn [c], Maureen H. Conte [d], William J. Cooper [e], David Bastviken [b], Ellen Druffel [f], Philippe Schmitt-Kopplin [c,g]

[a] University of MD Center for Environmental Science, Chesapeake Biological Laboratory, Solomons, USA
[b] Linköping University, Department of Thematic Studies — Water and Environmental Studies, Linköping, Sweden
[c] Helmholtz Zentrum Muenchen, German Research Center for Environmental Health, Neuherberg, Germany
[d] Bermuda Institute of Ocean Sciences, Ferry Reach, St. Georges GE01, Bermuda
[e] Urban Water Research Center, Department of Environmental and Civil Engineering, University of CA, Irvine, USA
[f] Department of Earth System Science, University of CA, Irvine, USA
[g] Department for Chemical–Technical Analysis, Research Center Weihenstephan for Brewing and Food Quality, Technische Universität München, D-85354 Freising-Weihenstephan, Germany

ARTICLE INFO

ABSTRACT

Ultrahigh resolution mass spectrometry of marine dissolved organic matter (DOM) has suggested the presence of many common molecular compositions throughout the open ocean. The majority of these supposedly ubiquitous molecules was concluded to represent the refractory marine DOM pool. This study demonstrates that 24 h of exposure of Atlantic and Pacific surface DOM to simulated sunlight causes phototransformation of about half of these supposedly refractory molecular compositions. It is suggested that these transformations are related to indirect photobleaching possibly involving reactive oxygen species (e.g. hydroxyl radicals), because very little change in the fluorescent component of the DOM (FDOM) was observed during the photo-degradation experiments. A significant decline in average mass with distinct decrease of average O/C ratios and concomitant increase of H/C ratios was observed. NMR spectra revealed a decrease in aromatic and olefinic unsaturation and the formation of a limited and near identical suite of oxygenated aliphatic compounds in both Atlantic and Pacific surface DOM. Their NMR characteristics indicated a mixture of about 10 polyols that are plausible products of convergent pathways of photochemical carbohydrate decomposition and oxidation of functionalized, branched aliphatic compounds. These prominent photochemical signature molecules amounted to ~2% of total proton NMR integral and are expected to be quickly consumed by various microorganisms in the open ocean. These results may suggest a fast photo-induced large-scale cycling of DOM within the surface ocean dynamic equilibrium of photo- and bio-transformations.

© 2014 Elsevier B.V. All rights reserved.

1. Introduction

Dissolved organic matter (DOM) is a very complex mixture of organic molecules and a key player in the global carbon and other elemental biogeochemical cycles. The global marine dissolved organic carbon (DOC) pool with 662 Pg carbon (Hansell et al., 2009) nearly equals the atmospheric CO_2 reservoir, but an estimated 80% of the carbon in marine DOM resides in molecules of unknown structure (Benner, 2002). The fundamental processes that control the production and cycling of oceanic DOM are still far from understood and current perception divides marine DOM into distinct pools termed labile, semi-labile and refractory, depending on their proposed average residence time (Carlson, 2002; Carlson and Ducklow, 1995). The euphotic/epipelagic ocean was estimated to hold about 7% of global oceanic DOC stocks (Hansell et al., 2009) and less than 50% of this surface ocean DOC may belong to the semi-labile DOC pool (Hansell et al., 2012), leading to suggestions that most of the DOC stock might be refractory. However, a steady-state situation, where compounds in a seemingly stable DOM pool are subject to a rapid turnover, would also conform to this view as explored in this study.

Commonly employed analytical methods lack the resolution to adequately cope with complex DOM (Hertkorn et al., 2007, 2013) and assessments of DOM production and cycling beyond bulk examination and coverage of small molecules (CO, CO_2, C_{3-4} units, common lipids) are consequently few. Ultrahigh resolution electrospray ionization Fourier transform ion cyclotron resonance mass spectrometry (FT-MS),

which allows identification of thousands of molecular formulae directly out of marine DOM, has recently enabled the detailed classification of marine DOM in various ecosystems (Flerus et al., 2012). For example, photochemical degradation of estuarine DOM resulted in significant molecular changes including an appreciable decrease in aromaticity (Gonsior et al., 2009; Stubbins et al., 2010). Transects from coastal to open ocean environments suggested an apparent decrease in numbers of mass peaks and their corresponding molecular formulae and preferential loss of terrestrial organic matter, as demonstrated, for example, in coastal New Zealand (Gonsior et al., 2011), the Chesapeake Bay (Sleighter and Hatcher, 2008) and the Congo River (Stubbins et al., 2010). Recent FT-MS analyses revealed an extended suite of common molecular compositions present in nearly all marine DOM (Flerus et al., 2012; Gonsior et al., 2011). These mass peaks and associated molecular formulae do not resemble any of the known common marine DOM components, such as polysaccharides (Benner et al., 1992), or more specifically acyl oligosaccharides (Aluwihare et al., 1997). The reason for this is probably the very weak ionization efficiency in electrospray of alcohols in general and saccharides in particular and the discrimination of the solid phase extraction (SPE) method used against highly polar compounds.

The near ubiquitous occurrence and congruent distribution patterns of certain molecular compositions in oligotrophic regions and throughout the entire ocean water column (Flerus et al., 2012) suggested their refractory character (Hansell and Carlson, 1998). These concepts were corroborated by radiocarbon analyses of marine DOC that proposed average ^{14}C ages of marine DOC ranging from tens to thousands of years depending on compound classes investigated and sampling location (Loh et al., 2004; Repeta and Aluwihare, 2006).

However, care must be taken when interpreting similarities in mass spectra as similarities in chemistry. Given the appreciable degree of unsaturation and content of heteroatoms (N, O, S) in marine DOM molecules, it is likely that several thousand isomeric molecules will project on any defined DOM molecular composition (Hertkorn et al., 2007). Therefore, even major structural alterations of marine DOM would not readily show up in high-resolution FT-MS spectra. In other words, the absence of spectral alterations does not necessarily indicate conformity of DOM molecular structures. In the case of marine DOM, even seemingly modest alterations of mass spectra would likely represent major changes in DOM chemistry. In particular, ever smaller mass differences between pairs of mass peaks imply an ever growing mandatory compositional and structural dissimilarity (Hertkorn et al., 2008).

Photochemistry is (together with redox chemistry) the most significant abiotic reaction in the surface ocean and supplies a sizable amount of energy into the surface ocean chromophoric dissolved organic matter (CDOM) (Mopper et al., 1991; Zafiriou et al., 2003). A dynamic equilibrium of loosely correlated abiotic and biotic production and degradation reactions governs the respective surface ocean DOM composition and structure. Hence, the surface ocean might be regarded as a continually operating gateway of biochemistry and photochemistry. Common photoreactions of surface ocean DOM refer to the loss of aromaticity and (conjugated) π-systems (Stubbins et al., 2012), with concomitant photo-production of oxidized aliphatic intermediates including carbonyl derivatives (mostly carboxylic acids) (Schmitt-Kopplin et al., 1998) and other low molecular carbon-based photoproducts such as CO and CO_2 (Mopper et al., 1991).

In the deep ocean, relatively fresh DOM supplied by the biological pump is consumed by hetero- or chemotrophic organisms and converted to biologically refractory DOM (Gruber et al., 2006; Ogawa et al., 2001), some of which is optically active (Yamashita and Tanoue, 2008) and photo-labile (Benner and Biddanda, 1998). Through upwelling and the meridional overturning circulation (MOC), the deep ocean DOM eventually reaches the surface again and supplies accumulated photochemically-reactive DOM to the "photochemical loop". A continuous photo-production of bioavailable marine DOM in the surface ocean would imply a dynamic equilibrium and a steady production or supply of photochemically active precursors to the surface that could be achieved through upwelling of deep-sea DOM as well as through the steady release of photochemically-active, microbial-derived DOM in the oligotrophic ocean. As a result, a dynamic equilibrium between photodegradation, biological consumption and excretion of photolabile compounds is feasible.

Knowing to what extent the apparent ubiquity of certain marine DOM molecules reflects arbitrary superposition of isomers, chemical identity and/or inertness or a dynamic equilibrium of interacting biotic and abiotic reactions with possibly different timescales is critical for our understanding of the ecological and biogeochemical roles attributed to marine DOM as one of the most dynamic pools in the global carbon cycle.

This study complements previous studies of DOM photomineralization in the surface ocean (Mopper et al., 1991) and gives a possible explanation of its photochemically-induced bioavailability (Benner and Biddanda, 1998; Kieber et al., 1989) by implementing ultrahigh resolution techniques such has FT-MS and high flied NMR. It presents data indicating rapid and large-scale photo-induced compositional and structural changes of SPE marine DOM (SPE-DOM) and the photoproduction of polyols from the oligotrophic surface Atlantic and Pacific Oceans following irradiation with simulated sunlight.

2. Materials and methods

2.1. Water sampling and sample preparation

Surface ocean water samples were collected using 12 L Niskin water samplers in summer 2009 within the North Pacific Gyre (140° 58.470 W; 38° 16.038 N) and in the Sargasso Sea/Atlantic Ocean (64° 5.000 W; 31° 55.000 N). In situ DOC concentrations at both stations were not measured but typical surface DOC concentrations in the Sargasso Sea as well as inside the North Pacific Gyre range from 70 to 80 μM (Hansell et al., 2009).

Each 20 L surface ocean water sample was filtered through pre-combusted (490 °C, overnight) Whatman GF/F glass fiber filters (0.7 μm), acidified to pH 2 and solid-phase extracted aboard the ships using the technique described elsewhere (Dittmar et al., 2008). Briefly, water samples were gravity-fed through 1 g Agilent Bond Elut PPL cartridges previously activated with methanol (analytical-grade, Chromasolv, Sigma-Aldrich). The PPL resin is made of a styrene–divinylbenzene (SDVB) polymer that has been modified with a proprietary non-polar surface. The adsorbed DOM was eluted with 10 mL LC–MS methanol and stored at −20 °C prior to further analysis; typical extraction efficiencies of this specific SPE method were shown to range near 60% of the DOC, superior to, e.g. ultrafiltration (Dittmar et al., 2008). Elaborate instrumentation such as the combination of reversed osmosis membranes and electrodialysis (Gurtler et al., 2008) has provided better DOM recovery, but the PPL method employed here provided advantages that included adequate field work capability, appreciable yield and excellent observability in organic structural spectroscopy (Hertkorn et al., 2013). The recovered SPE-DOM was also easy to dry and it was completely re-dissolved in pure water and deuterated methanol (CD_3OD). Relatively polar compounds (e.g. phenols) were still retained and eluted from PPL. It is assumed that some low molecular weight highly polar compounds, such as (poly-) acids, are not fully recovered, but these compounds are often too small to be analyzed by current FT-ICR mass spectrometry.

2.2. Photochemical experiments

To assess the photochemical changes in the molecular composition of DOM by mass spectrometry and nuclear magnetic resonance (NMR) spectroscopy, SPE was necessary to desalt and concentrate marine DOM. This SPE procedure alters the marine DOM matrix and removes seawater constituents such as trace metal ions that are potentially important photochemically. Trace metals are still present in SPE-DOM (Hertkorn et al., 2013). However, metal ions are probably coordinated

to SPE-DOM. Indeed, the near absence of trace metal ions and other open ocean constituents implies a more conservative photo-degradation, because it is likely that trace metals would function as catalysts and hence would enhance photochemical reactions. Furthermore, SPE following the exposure to simulated sunlight had to be avoided to be able to evaluate the production of smaller highly polar molecules. These compounds would have otherwise escaped detection and the only viable means to track a more complete picture of DOM molecular transformation was to perform all photochemical experiments in pure water.

Two milliliters of the methanolic SPE-DOM solutions was dried under nitrogen gas and completely re-dissolved in pure water (analytical-grade, Chromasolv, Sigma-Aldrich). The Raleigh scattering, while measuring EEM spectra, was as low as that in Milli-Q water indicating that the dried SPE-DOM was fully dissolved. Half of the re-dissolved SPE-DOM solution was continuously pumped through a custom-built flow cell made of Tefzel (ethylene tetrafluoroethylene, ETFE, with >90% transmittance at 300 nm) tubing with a diameter of 1 mm for 24 h and a gas equilibrator (20 mL vial, 95% volume of air) while exposed to simulated sunlight (Solsim Luzchem) and a 250 W xenon light source.

The intensity of the light source was very similar (<0.01% total difference) to the reference spectral distribution of sunlight by using the global Air Mass 1.5 (AM 1.5) filter (SolSim Luzchem). The irradiance matched one sun at noon in summer at mid-latitudes (870 W m^{-2}) and an insolation of about 20.9 kWh was achieved during our 24 h exposure. The daily insolation at August in Bermuda is 20.9 MJ or 5.8 kWh (Zafiriou et al., 2008). Assuming 100% transmission, the 24 h irradiation time used in our experiments would translate into about 3.5 days of surface insolation in the Sargasso Sea. Although the exact irradiance within the Tefzel tubing is not known, a 10% lower level is likely based on the transmittance of the Tefzel tubing of 90% at 300 nm. This estimate is purely based on the insolation and completely neglects processes such as mixing.

This photodegradation system eliminates inner filtering effects (very short path length), avoids starvation of oxygen (sample is continuously dripping through air in equilibrator) and reduces possible contamination (closed system). Adsorption processes on the tubing walls were negligible as shown by previous experiments with no obvious effects (data not shown). The other half of the sample was used as a dark control and stored at ambient room temperature (similar ± 3 °C to the 25 °C maintained inside the solar simulator) in the dark. DOC measurements were not performed because they are not sensitive enough to depict very small changes in DOC and the presumably very low DOC photo-mineralization rates during the short 24 h irradiation time. On the other hand, fluorescence, NMR and FT-MS are much more sensitive in tracking changes within the molecular moieties below the level of mineralization.

2.3. Measurements of optical properties

Ultraviolet–visible (UV–vis) absorption spectra and excitation emission matrix (EEM) fluorescence spectra were measured for all SPE extracted and re-dissolved SPE-DOM samples (SPE-DOM fully re-dissolved in pure water, pH 6.6) before and after exposure to simulated sunlight using a Cary BIO 100 UV–vis spectrophotometer and a Yvon Horiba Fluoromax-4 Spectrofluorometer, respectively. The raw optical densities (A) of the UV–vis spectra were normalized to the pathlength and calculated to apparent absorption coefficients (a) according to a previous study (Gonsior et al., 2008). The EEM spectra were scatter-corrected and normalized to the fluorescence of quinine sulfate. A detailed description of the procedure is described elsewhere (Zepp et al., 2004).

2.4. Ultrahigh resolution mass spectrometric analysis

Mass spectrometry of all SPE-DOM was performed using a Bruker Apex QE 12 Tesla ESI-FTICR mass spectrometer. An aliquot of 10 μL of the SPE-DOM solution was diluted 1:20 with LC–MS grade methanol

(Sigma-Aldrich Chromasolv, LC–MS methanol) and then injected at a flow rate of 2 μL/min. The electrospray ionization was run in negative ion mode and the ion accumulation time was optimized to not overload the ICR cell. Transient spectra were within the expected range and indicative for a non-saturated ICR cell. To obtain robust and accurate results, 1000 scans were averaged. All mass spectra were internally calibrated using known mass peaks commonly found in marine NOM (Gonsior et al., 2009, 2011).

The resolution achieved (typically <200 ppb mass uncertainty) was sufficient to compute unambiguous molecular formulae from m/z peaks (Stenson et al., 2003). Calculations for the exact molecular formulae were based on the following chemical elements: $^{12}C_{0-\infty}$, $^{1}H_{0-\infty}$, $^{16}O_{0-\infty}$, $^{14}N_{0-5}$ and $^{32}S_{0-2}$ as well as the ^{13}C isotopologue. A comprehensive description of the procedures to accurately assign molecular formulae of ultrahigh resolution FT-MS data is given elsewhere (Koch et al., 2007).

Van Krevelen diagrams represent an effective visualizing tool for large numbers of molecular formulae (Hertkorn et al., 2008; Kim et al., 2003). Unsaturation of molecular formulae can be classified by means of Double Bond Equivalency (DBE). DBE provides counts of C=C and C=O double bonds as well as numbers of alicyclic rings present in molecular compositions. In a previous study, the aromaticity index (AI) was introduced (Koch and Dittmar, 2006). Based on ^{13}C NMR spectra obtained for open ocean SPE-DOM (Hertkorn et al., 2013), about 1/7 (15%) of the oxygen in SPE-DOM is present in carbonyl and its derivative groups (mainly COOH). A modified AI (AI_{mod}) would provide an adequate estimate of the double bonds remaining within the carbon skeleton:

$$AI_{mod} = (1 + C - O/7 - S - H/2)/(C - O/7 - S - N - P) \qquad (1)$$

For more straightforward visualization in a single graph and comparison, we previously proposed a new diagram: the KMD-z* mass plot (Shakeri Yekta et al., 2012). The Kendrick mass defect (KMD) and the z* values are independent parameters to unambiguously identify homologous series (Stenson et al., 2003).

$$Kendrick\ Mass(KM) = mass_{measured}(14.0000/14.01565) \qquad (2)$$

$$KMD = nominal\ mass\ (NM) - KM \qquad (3)$$

$$z^* = modulus(NM/14) - 14 \qquad (4)$$

We divided KMD by z* and plotted this ratio against the exact mass. The resulting diagram spreads respective molecular compositions across larger areas than standard Kendrick diagrams and therefore shows improved apparent resolution of molecular compositions. Within the C,H,O-compositional space, homologous series of H_2-spacing ($\Delta m = 2.1057$ Da), CH_2-spacing ($\Delta m = 14.0156$ Da), and the spacing created by the formal exchange of CH_4 against oxygen ($\Delta m = 36.4$ mDa) are nicely separated (see also SI Fig. S3a and b).

The reproducibility of all mass spectra was computed based on the relative error of all mass peak intensities of triplicate samples, and on average, the intensities did not vary more than 4%. The absolute intensities were used for (statistical) analysis because scaling the mass spectrum to the highest peak (rel. abundance) could have introduced systematic errors, and it was not clear if the most abundant mass peaks also underwent photochemical changes.

2.5. Nuclear magnetic resonance spectroscopy

NMR spectra were acquired immediately after sample preparation using a Bruker Avance III spectrometer operated at 500.13 MHz ($B_0 = 11.7$ T) and TopSpin 3.0/PL3 software. For analysis, SPE-DOM was redissolved (40–150 μg solid DOM in typically 50–75 μL CD$_3$OD (99.95% ^{2}H; $\delta_{H/C} = 3.30/49.0$ ppm), Aldrich, Steinheim, Germany) and sealed in 2.0 mm Bruker Match tubes. An inverse geometry 5 mm z-gradient ^{1}H/^{13}C/^{15}N TXI cryogenic probe (90° excitation pulses:

$^{13}C \sim {}^{1}H \sim 10 \,\mu s$) was used to impede side reactions during NMR acquisitions. A comparison of ^{1}H NMR spectra acquired before and after lengthy acquisitions showed negligible alterations. 1D ^{1}H NMR spectra were recorded with a spin-echo sequence (10 μs delay) to allow for high-Q probe ring down, and classical pre-saturation. The one bond coupling constant $^{1}J(CH)$ used in ^{1}H and ^{13}C distortionless enhancement by polarization transfer heteronuclear single quantum coherence spectroscopy (DEPT-HSQC) spectra was set to 145 Hz; F2 (^{1}H): spectral width of 5981 Hz (11.96 ppm), 250 ms acquisition time; 1.25 s relaxation delay and F1 (^{13}C): SW = 17,607 Hz (140 ppm). HSQC-derived NMR spectra were computed to a 4096 × 512 matrix. Gradient (1 ms length, 450 μs recovery) and sensitivity-enhanced sequences were used for DEPT-HSQC and correlation spectroscopy (COSY) NMR spectra. Absolute values of J-resolved COSY and phase-sensitive echo–antiecho total correlation spectroscopy (TOCSY) spectra (70 ms mixing time, with solvent suppression) were obtained using a spectral width of 5498 Hz [JRES (F1) = 50 Hz] and were computed using a 8192 × 2048 matrix (JRES (F1) = 128). Additional NMR acquisition conditions are given in Supporting Information Table S1.

3. Results and discussion

The photochemical experiments of marine surface SPE-DOM showed that the absorbance (Fig. S1a) and EEM fluorescence did not substantially changed (Fig. S1b), but FT-MS and ^{1}H NMR data revealed fundamental phototransformations. A mass shift to lower masses and more saturated compounds was observed at each nominal mass in the FT-ICR mass spectra (Figs. 1–3) as well as the surprising photo production of extensively oxygenated aliphatic molecules (polyols) confirmed by ^{1}H NMR (Figs. 4 and 5).

3.1. Optical properties

Changes in UV–vis absorption after illumination were minimal (Fig. S1a) and reflected the already photobleached nature of surface ocean DOM, although some absorption in the photo-active region of sunlight (≥300 nm) remained. The EEM fluorescence of Pacific Ocean and Atlantic Ocean surface SPE-DOM samples suggested the presence
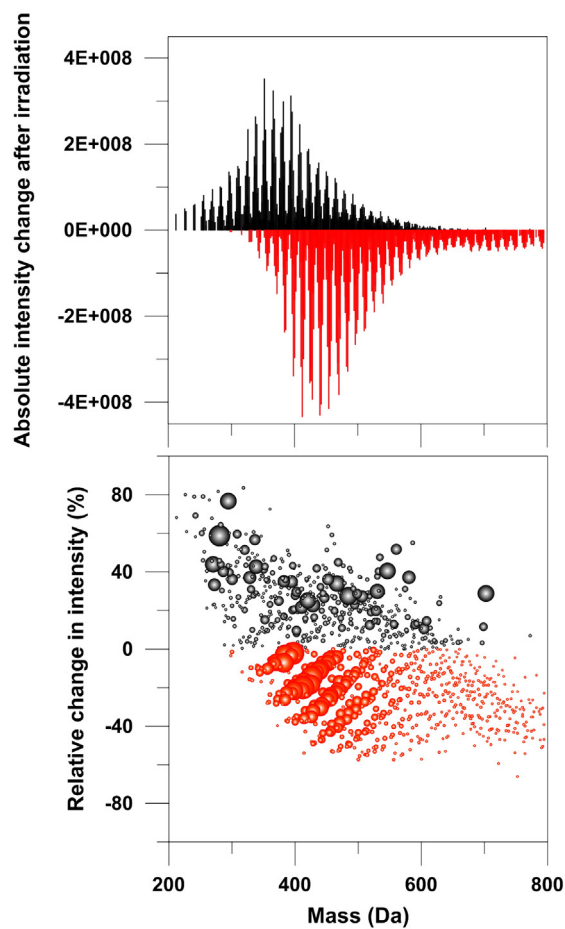

Fig. 2. Absolute and relative intensity differences of the consolidated Pacific (PAC) and Atlantic (ATL) surface ocean SPE-DOM (ATLPAC) before (blue) and after (red) 24 h solar irradiation between 200 and 800 Da. Note: bubble size represents relative abundance of mass peaks after irradiation. (For interpretation of the references to color in this figure legend, the reader is referred to the web version of this article.)
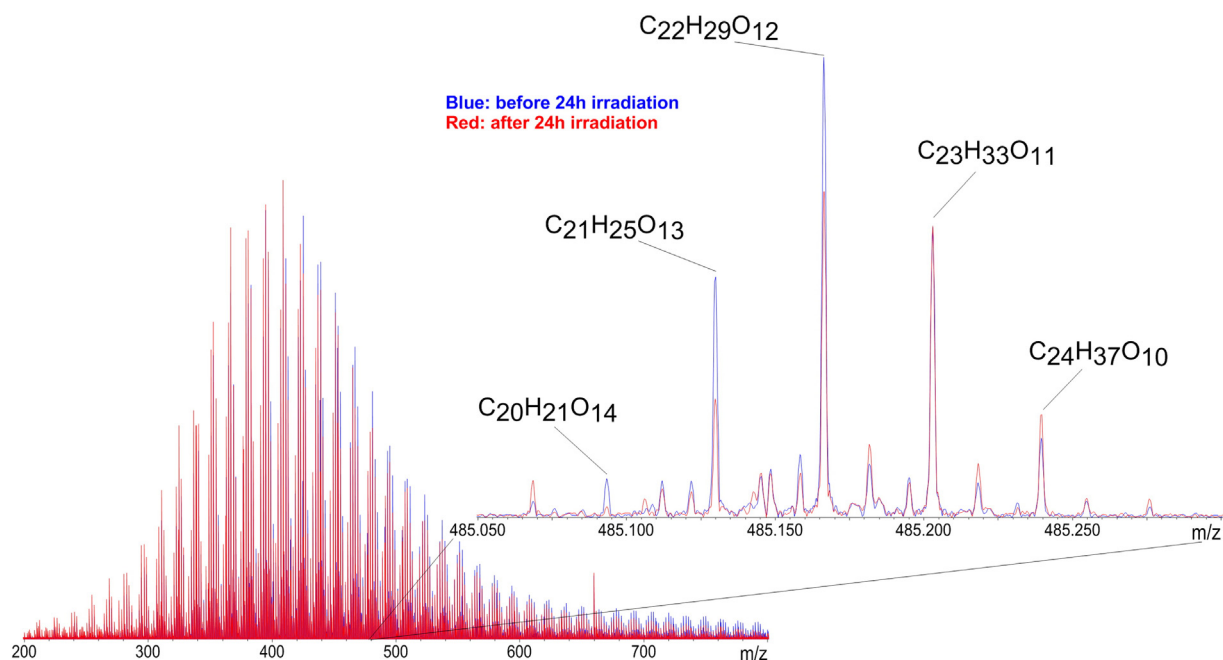

Fig. 1. Overlaid mass spectra of surface Pacific Ocean SPE-DOM before and after the exposure to 24 h of simulated sunlight. The clear shift from mass peaks that resemble high oxygen content molecular formulae to lower oxygen bearing molecules is clearly visible at each nominal mass (NM) and demonstrated here at NM 485.
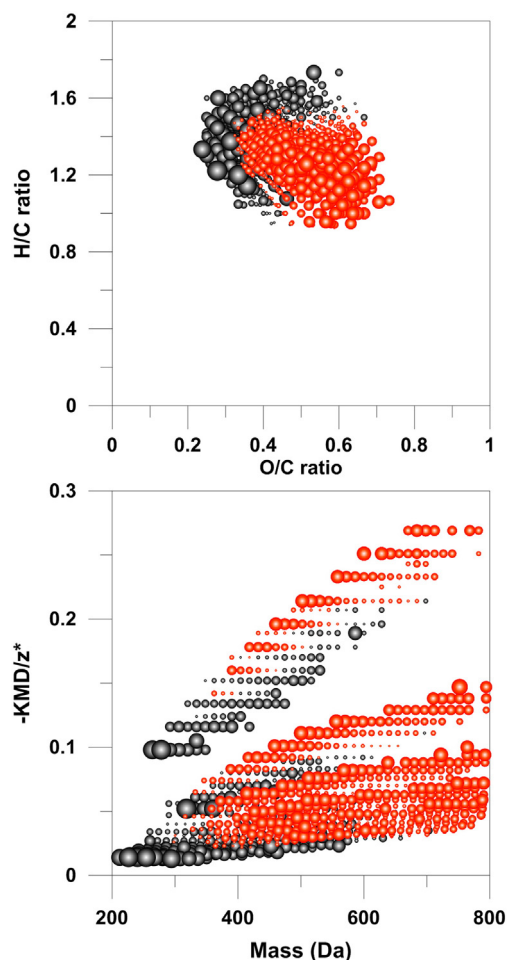
Fig. 3. Van Krevelen diagram of decreased and increased relative abundances of molecular formula assigned mass peaks after irradiation. Note: size of bubbles represents the relative change in intensity in percent of associated mass peaks with black being increased and red being decreased. Photo-induced large scale mass distribution shifts at each homologous series are visualized using the KMD-z* plot (Shakeri Yekta et al., 2012). (For interpretation of the references to color in this figure legend, the reader is referred to the web version of this article.)

Fig. 4. ^{1}H NMR spectra (500 MHz) of aliphatic section (δ_H: 5–0 ppm) of Atlantic surface ocean (ATL), Pacific surface ocean (PAC) and consolidated (ATLPAC) SPE-DOM in CD$_3$OD before and after photo irradiation (see also Figs. 6, S4, S5 and S7).

of marine fluorescent DOM (FDOM) (Fig. S1b) that has not been reported, likely because concentrations are too low to be directly analyzed in open ocean environments, and fluorescent analyses on isolated marine SPE-DOM are rare. The slightly lower pH of 6.6 in the re-dissolved sample may have caused some shifts in peak area and/or intensity when compared to ambient seawater pH but this conceivable shift cannot explain the overall observed fluorescence. The EEM fluorescence before exposure can partly be explained by protein-like DOM with maxima located at the excitation/emission (ex/em) pairs: 250/325 nm and 270/325 nm (Fig. S1b), but fluorescence peaks at emission wavelengths >350 nm are outside the fluorescence of the known fluorescent amino acids (tryptophan, tyrosine) and represent unknown fluorescent marine DOM.

Fluorescence properties of the SPE-DOM showed very little change after 24 h exposure to simulated sunlight indicating an appreciable photo-stability except for a limited (<2%) loss of FDOM at emission λ < 300 nm caused by indirect photolysis.

3.2. Ultrahigh resolution mass spectrometry

ESI-FT-ICR mass spectra of both Atlantic and Pacific surface marine SPE-DOM before and after exposure to simulated sunlight showed large and nearly identical changes indicative of significant photo-degradation (Fig. 1). The remarkably similar photochemistry of Atlantic
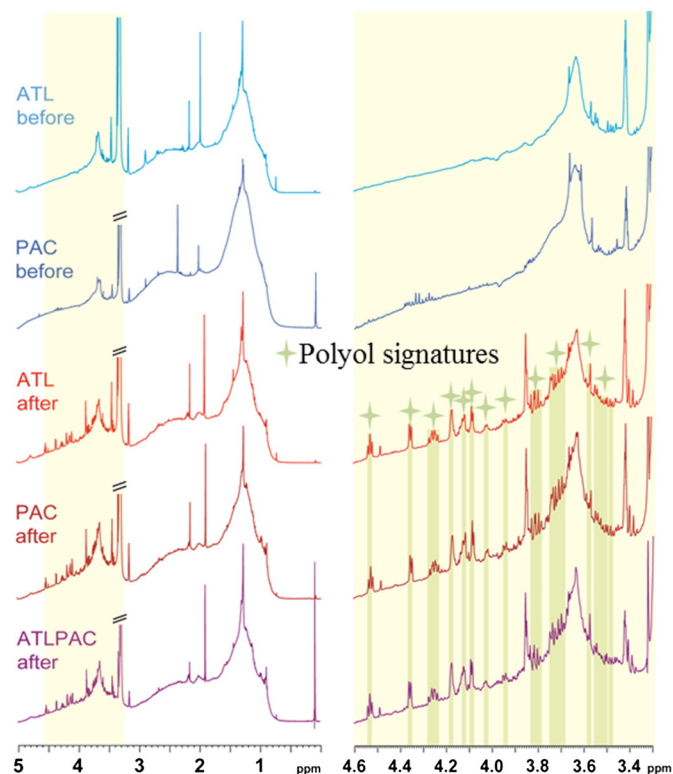
and Pacific SPE-DOM, that allowed averaging for a more robust analysis, suggested a near accordance of molecular compositions as represented by mass peaks. A strong resemblance, with respect to their underlying photo-reactivity, was also observed and indicated conformity of certain molecular structures. The strong vertical stratification of the upper water column in the sampling regions could support the accumulation of DOM resistant to biological degradation (Hansell et al., 2009) and the FDOM observed in this study might be part of that pool.

Both, absolute and relative photochemically-induced changes (Figs. 1 and 2) resulted in a systematic decrease in intensity (up to 60%) of mass peaks representing large molecules (m > 300 Da) whereas those associated with smaller molecules (m < 500 Da) grew up to 90% in mass peak intensity. This photo-induced shift from higher to lower masses for ubiquitously distributed molecular compositions has previously been observed in a coastal to open ocean DOM study (Gonsior et al., 2011) and along an estuarine transect (Dalzell et al., 2009). The change in the apparent molecular weight distribution was accompanied by remarkably systematic intensity variations of mass peaks within each nominal mass (Fig. 1), and reflects a displacement from relatively oxygen-rich and hydrogen-deficient compositions towards those with lower oxygen and higher hydrogen content (Table 1, Figs. 3, S2). The C,H,O molecular series that underwent significant intensity variations following photo-degradation in this study had been also observed in all FT-ICR mass spectra of marine DOM (Flerus et al., 2012; Gonsior et al., 2011) but were assumed to represent the refractory DOM pool in the oceans.

In complex mixtures such as marine DOM, mass peak displacements have to overcome massive intrinsic averaging, and any spectral change will reflect major compositional and structural alterations (Hertkorn et al., 2008, 2013). Hence, the observed intensity variations of mass peaks during the photochemical degradation experiments strongly suggest major molecular changes of the marine DOM or less likely, a more restricted isomeric diversity of marine DOM than currently believed.
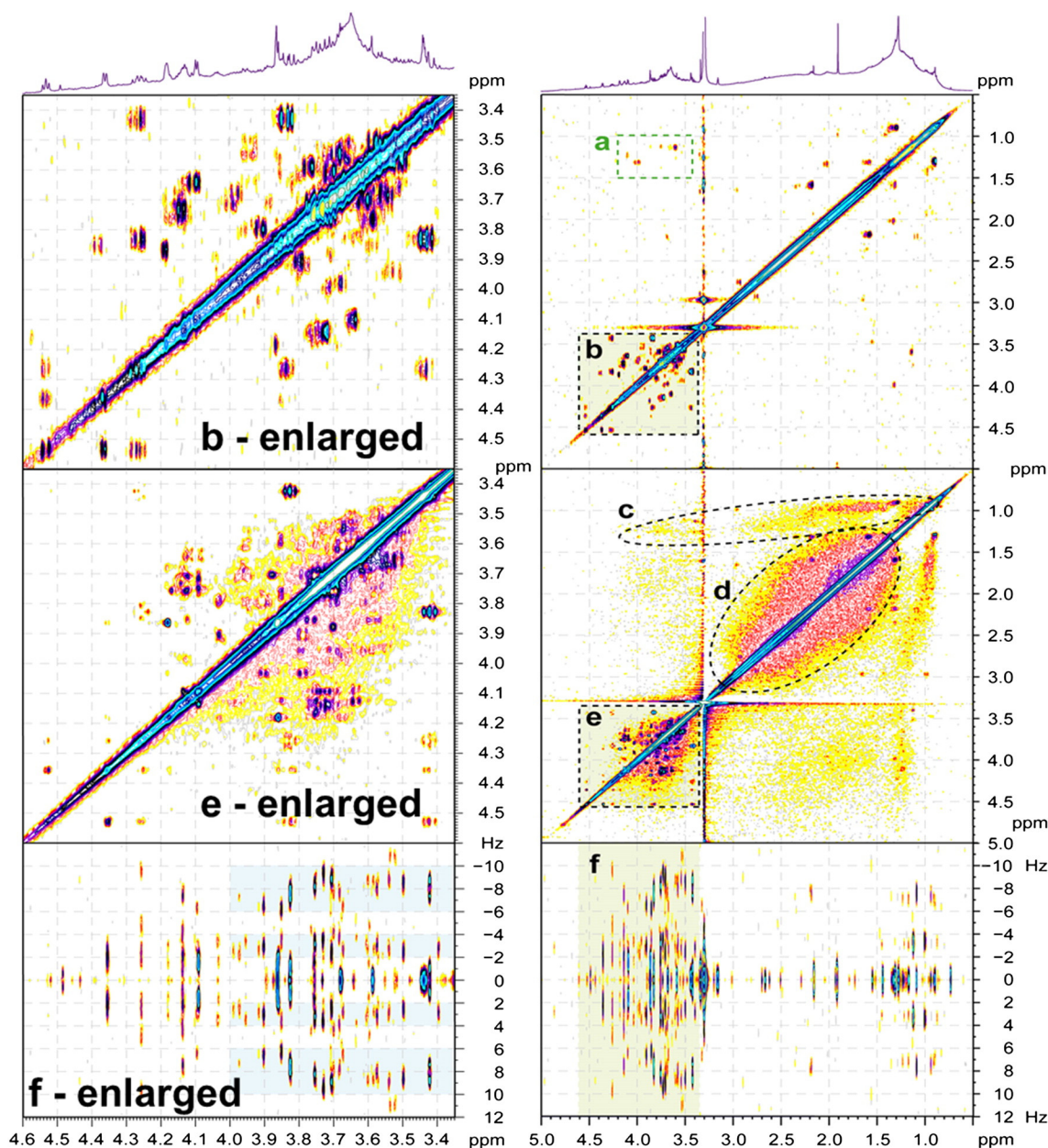
Fig. 5. ^{1}H NMR spectra (500 MHz) of the consolidated Atlantic and Pacific SPE-DOM after photolysis; top: ^{1}H, ^{1}H COSY, middle: ^{1}H, ^{1}H TOCSY and bottom: ^{1}H JRES NMR spectra. Box a: the relative insignificance of aliphatic $C-\underline{H}C-C\underline{H}-O$ COSY cross peaks implies near absence of partially oxygenated aliphatic compounds and dominance of polyol derivatives; box b, e, f: areas of $O-C\underline{H}-C\underline{H}-O$ substructures shown in respective left panels; box c: $\underline{H_3}C-C\underline{H}-X$ TOCSY cross peaks related to chain-terminating methyl groups; for $\delta_H > 3$ ppm: with oxygenated carbon $\underline{H_3}C-C\underline{H}-O$; box d: intra aliphatic TOCSY cross peaks excluding methyl ($Z-C-C\underline{H}-C\underline{H}-C-Z$; Z: O, N), often in carboxyl-rich alicyclic molecules CRAM (Hertkorn et al., 2006, 2013).

The presumably photo-refractory marine DOM pool (represented by mass peaks with retained or increased amplitude after irradiation) was significantly smaller than previously assumed and confined to a rather restricted range of O/C and H/C ratios, being more saturated and oxygen-deficient than photo-labile marine DOM (Figs. 3 and S2). The photo-sensitive component was not significantly correlated with optical properties indicated by practically unchanged fluorescence during irradiation (see Fig. S1). One may argue that photochemical alterations of some compounds in a complex mixture drastically change the charge competition within the electrospray, but that seems very unlikely given the experimental conditions of dilute samples (prior to mass spectrometric analysis, all samples were diluted 1:20) and the consistent drastic congruent shift at each nominal mass across the entire observed mass range.

Photo-degradation of marine SPE-DOM could have been initiated by energy transfer from the CDOM/FDOM (see Fig. S1) to conjugated π-electrons and carbonyl derivatives (i.e. ketones, CONH, COOH and COOR derivatives), followed by less selective "general attack" from reactive oxygen species such as hydroxyl radicals, singlet oxygen and hydrogen peroxide (Schmitt-Kopplin et al., 1998; Shank et al., 2010; Wang et al., 2007). All photochemical experiments were undertaken in pure water and as a result the photo-production of hydroxyl radicals from nitrate (Calza et al., 2012; Zepp et al., 1987) could not occur. On the other hand, scavenging of the hydroxyl radical by primarily bromide was also prevented (Zafiriou Oliver et al., 1987).

Photo-extrusion of thermodynamically stable oxygen-rich molecules like H_2O, CO, and CO_2 could explain the overall decrease in O/C and increase in H/C ratio in residual SPE-DOM after oxidation also

Table 1
Descriptive FT-MS analysis of consolidated Atlantic and Pacific surface ocean SPE-DOM, with photo-refractory and photo-labile C,H,O-molecular compositions indicated; percent ^{1}H NMR section integrals (exclusion of the residual water and methanol) are given according to key substructures (for individual samples: see Supporting Information).

Item	Photo-refractory C,H,O-molecules		Photo-labile C,H,O-molecules
n	513		616
Center of mass	417.6 ± 15.7		495.5 ± 16.4
O/C ratio	0.41 ± 0.003		0.50 ± 0.005
H/C ratio	1.36 ± 0.005		1.28 ± 0.002
DBE	7.75 ± 0.18		9.40 ± 0.32
DBE/C	0.37 ± 0.004		0.41 ± 0.0005
Almod	0.3003 ± 0.0052		0.3237 ± 0.0004
δ^1H [ppm]	Main substructure	Marine NOM before irradiation [%]	Marine NOM after irradiation [%]
10–7	$\underline{H}_{ar}$	1.4	0.8
7–5.3	$\underline{H}_{ar}$ and $C=C\underline{H}$	1.5	0.8
4.9–3.1	$OC\underline{H}$	21.4	24.0
3.1–1.9	$X^*C\underline{C}\underline{H}$, $X^*CCC\underline{H}$	30.3	27.8
1.9–0.0	$CC\underline{H}$	45.4	46.6

Note: all FT-MS-derived parameters were weighted by intensity prior to statistical analysis and all errors (standard error of mean = SEM) are derived from averaging the two separate photo-degradation experiment results; (*) X denotes heteroatom, commonly oxygen.

observed in previous studies (Einsiedl et al., 2007; Schmitt-Kopplin et al., 1998). Here, an average loss of 1.5 to 2 CO_2 molecules per molecular composition for masses >300 Da could account for the observed displacement in O/C and H/C ratios. Partial photo-mineralization within larger functionalized SPE-DOM molecules will also result in lesser average molecular weight. These results are supported by a previous study measuring the photochemical production of CO_2 from marine DOM (Wang et al., 2009). z*-normalized Kendrick mass analysis (Figs. 3, S3a and b) demonstrated the presence of separate and extended homologous C,H,O-molecular series (based on CH_2), suggesting prevailing structural similarities specific for the respective photo-labile and for the photo-refractory SPE-DOM pools (Fig. S3c and d).

3.3. Nuclear magnetic resonance spectroscopy

Pacific and Atlantic surface ocean SPE-DOM provided bulk ^{1}H NMR signatures with a more pronounced downfield shoulder of methyl esters at the shift of $\delta_H > 3.7$ ppm in the Pacific DOM (Figs. 4 and S4). However, the ^{1}H NMR signals from the Atlantic and Pacific surface ocean showed only minor differences. The better resolved ^{1}H NMR spectra from the Atlantic DOM suggested a slightly higher abundance of presumably biologically-derived organic molecules than in the Pacific (Figs. 4 and S4). Twenty-four hours of photo irradiation imposed rather marginal bulk changes of saturated (sp^3 hybridized) organic carbon in ^{1}H NMR spectra in line with the extensive previous exposure of surface marine DOM to high levels of natural sunlight in the surface ocean. Narrowing of ^{1}H NMR resonances of SPE-DOM photoproducts was indicative of smaller organic molecules present, in line with lesser molecular weight observed in the FT-ICR mass spectra of SPE-DOM photo-products after irradiation. Aromatic and olefinic unsaturation in SPE-DOM photo-products decreased by nearly one half (Table 1).

A remarkable suite of distinct ^{1}H NMR signals appeared following photoirradiation, primarily in the $\underline{H}C-O$ section (δ_H: 3.5–4.6 ppm). The specific signature of oxygenated aliphatic compounds in Pacific and Atlantic SPE-DOM nearly coincided, suggesting the presence of a common suite of about 10 photo-produced molecules (see Fig. 4) that accounted for ~2% of the total ^{1}H NMR integration (Table 1, Figs. 4, S4). The extensive accordance of Pacific and Atlantic SPE-DOM photoproducts even allowed pooling of samples for consecutive acquisition of 2D ^{1}H NMR spectra (Table S1, Figs. 5 and S5). Intense and well separated 2D ^{1}H NMR cross peaks (Figs. 5, S5, S6) also indicated photo-production of a limited series (≤10 compounds) of oxidized aliphatic compounds (δ_H: 3.5–4.6 ppm). The near absence of $-C-C\underline{H}-C\underline{H}-O$ COSY cross peaks of the photo-products (Fig. 5, box a) showed that almost all of its aliphatic carbon resided in HCO-

units. J-resolved NMR spectra of photo-degraded SPE-DOM in the range of δ_H ~ 3.5–4.0 ppm ($\underline{H}$CO-units) were dominated by about 20 conspicuous cross peak patterns with similar "double-doublet" (dd) splittings in ^{1}H NMR spectra with frequencies of $^nJ_{HH}$ ~ 6 Hz and $^nJ_{HH}$ ~ 12 Hz (Fig. S6). The combined action of one vicinal ($^3J_{HH}$ ~ 6 Hz) and one geminal ($^2J_{HH}$ ~ 12 Hz) coupling would cause a dd-splitting in excellent agreement to the observed JRES cross peak patterns (Fig. S6; $^2J_{HH}$ for methanol: 10.8 Hz (Pretsch et al., 2009)) and would indicate that these photo-products are extensively oxygenated aliphatic compounds.

Photo-induced ring opening reactions of saccharides in SPE-DOM (Schuchmann and von Sonntag, 1977) would result in lower molecular diversity and polyol production. A convergent photochemical synthesis of open chain polyols from ring opening of saccharides (Schuchmann and von Sonntag, 1977) and oxidation of functionalized aliphatic compounds (Schmitt-Kopplin et al., 1998) present in original marine SPE-DOM would result in a reduced overall molecular diversity from the loss of small carbon-based fragments (like CO and CO_2). JRES, COSY and DEPT HSQC NMR cross peaks of photo-products of surface ocean SPE-DOM did not exactly conform to those of selected prospective C_3–C_6 polyols (Figs. 4, 5, S5–S7) but shared important NMR characteristics, including downfield ^{13}C chemical shift of oxomethylene cross peaks (δ_H/δ_C: 63–65 ppm/3.5–3.7 ppm, and δ_H/δ_C: 61–63/3.7–3.8 ppm) and a narrow bandwidth of δ_C for methine HCO-units (71 ± 2 ppm for δ_H ~ 3.6–4.0 ppm, more uniform than common sugars) (Breitmeier and Voelter, 1989). Chain terminating spin systems likely produced the most prominent JRES cross peaks at δH~3.6-–4.0ppm (Figs. S6 and S7).

Hence, polyols in conceivable conjunction with carboxylic acids and ester groups (to accommodate for ^{1}H NMR resonances with $\delta_H > 4.0$ ppm) were in excellent agreement with all proton NMR chemical shift data of HCO-units in photo-degraded surface ocean SPE-DOM. The remarkable abundance of a few (≤10) oxidized aliphatic photochemical signature molecules speaks in favor of a convergent synthesis from several different precursor molecules present in common SPE-DOM. Polyols, with their absence of π-electrons, are not overly photo-reactive but might be readily bioavailable (common polyols often occupy gateway positions in metabolic maps). When quickly consumed under natural conditions then they would presumably never exceed a barely-detectable threshold abundance in any real world surface oceanic environment. However, it was not clear if polyols would be efficiently extracted by the SPE method used in this study.

In order to assess the extraction efficiency of photochemically-produced polyols, the consolidated Atlantic and Pacific SPE-DOM in D_2O was processed again by SPE using a 100 mg PPL cartridge while

500 MHz proton NMR spectra served to assess the chemical selectivity of extraction (Fig. S8). The photo-produced polyols of the consolidated Atlantic and Pacific photo-irradiated SPE-DOM were fully soluble in D_2O (Fig. S8B). Nevertheless, the photo-produced polyols were largely absent in the PPL methanol eluate (Fig. S8C), suggesting its low extraction efficiency with the PPL resin. Analogous limited trapping efficiency was observed for related polar natural products and comparable SPE cartridges (Clarkson et al., 2007). This retention behavior supports the original structure proposed from the NMR spectra. Notably, recognizable NMR signature molecules were only produced within the chemical shift range of singly oxygenated aliphatic compounds ($\delta_H \sim 3.3$–4.7 ppm). However, no NMR signatures with equivalent amplitudes and integrals appeared in the aliphatic section ($\delta_H < 3$ ppm) and in the section of unsaturated protonated carbon ($C_{sp2}\underline{H}$; $\delta_H > 5$ ppm). Similarly, COSY cross peaks indicating O$-$C$\underline{H}-$C$\underline{H}-$C units were nearly absent as well (Fig. S5). Therefore, aliphatic esters RCOOR′ with contiguous aliphatic residues larger than C_2 could be excluded as relevant photoproducts of marine SPE-DOM. While it is unambiguous that polyols have been photochemically-produced from marine SPE-DOM, its previous abundance in oligotrophic surface ocean waters is less constrained. We therefore cannot rule out that these polyol-like components were present in the surface ocean at unknown concentrations.

While polyols in general are considered slightly digestible carbohydrates, it has been previously established that fermentation in the large intestine of humans (Coudray et al., 2003) effectively degrades most polyols by the microbial assemblage in the gut to yield short chain fatty acids (Livesey, 1992, 2003). Additionally, polyol-specific long-chain dehydrogenases/reductases are well characterized (Krahulec et al., 2009) and the involvement of polyols in metabolic pathways of algae was also previously demonstrated (Iwamoto and Shiraiwa, 2005). With the current exception of erythritol, all common sugar alcohols occupy critical positions at common metabolic pathway maps such as the Kyoto Encyclopedia of Genes and Genomes (KEGG), suggesting that small, polar and ubiquitous polyhydroxylated molecules with their susceptibility to effective fermentation and involvement in metabolomics pathways will be readily degraded by adapted surface ocean microbial populations. However, at this stage the bioavailability of polyols by marine microbial communities is unknown, but given their rather small size, molecular structure, their susceptibility to effective fermentation and involvement in metabolomics pathways, our assumption that they are quickly biodegraded in surface ocean water seems plausible.

The degree of photo-degradation in oligotrophic surface ocean settings is largely defined by the light penetration and the photo-reactivity of organic matter. Quantitative analysis of mineralization rates (as derived from CO production) suggested that open ocean photochemistry affects DOC mineralization of 47 Tg CO carbon per year (Stubbins et al., 2006). This amount however only reflects a minimum direct DOC photo-mineralization and cannot assess photochemically/biologically controlled fast change (cleavage and rearrangements) in molecular moieties. Assuming a standard exposure of 62 J cm^{-2} day^{-1} of broad band UV light (Zafiriou and True, 1979) and an average photochemically-active depth of 5 m for photochemical mineralization of DOC (Mopper et al., 1991), it is likely that less energetic but deeper penetrating radiation can still induce photochemical changes of marine DOM molecular structures below the level of partial and total mineralization. It is also well established that indirect photolysis either via energy transfer or the involvement of reactive oxygen species (ROS) can yield molecular changes that otherwise would not be possible based on the energy (wavelength) of the utilized light alone. Furthermore, long-term (>50 days) photo-degradation experiments of Congo River DOM also showed photo-degradation of carboxyl-rich alicyclic molecules (CRAM) that had been considered relatively inert (Stubbins et al., 2010). As a result, photochemically-induced molecular changes of marine organic matter are plausible within a large surface volume of open ocean environments.

4. Conclusions

The integration of ^{1}H NMR spectra provided about 2% of "polyol-signature molecules". While this seems low, this set of about 10 compounds is similar to the abundance of major amino acids identified in all surface marine DOM (Benner, 2002). Therefore, these fully oxygenated aliphatic compounds are key photochemical surface ocean signature molecules of presumably ubiquitous abundance (Figs. S4, S6). In the context of possibly millions of molecules present in surface marine DOM, an about 2% contribution of these few polyol-type compounds to the overall NMR integral is remarkable.

Our study suggests an underestimation of solar irradiation effects in DOM turnover in the surface ocean, as up to half of the supposedly ubiquitous and generally considered recalcitrant DOM molecular compositions, analyzed by FT-MS, were found to be photo-transformed. Hence, much of the supposedly bio-refractory DOM present in the world's oceans could be readily photo-transformed into presumably more bio-labile and/or otherwise reactive compounds.

The finding of a close relationship between photochemical degradation and production of presumably bioavailable organic molecules in the surface ocean demonstrates the necessity to supplement traditional, established optical methods of marine DOM characterization with ultra-high resolution techniques. This study invites to reassess the nature and extent of refractory organic matter in the world's oceans.

Appendix A. Supplementary data

Supplementary data to this article can be found online at http://dx.doi.org/10.1016/j.marchem.2014.04.002.

References

Aluwihare, L.I., Repeta, D.J., Chen, R.F., 1997. A major biopolymeric component to dissolved organic carbon in surface sea water. Nature 387 (6629), 166–169.
Benner, R., 2002. Chemical composition and reactivity. In: Hansell, D.A., Carlson, C.A. (Eds.), Biogeochemistry of Marine Dissolved Organic Matter. Academic Press, pp. 59–90.
Benner, R., Biddanda, B., 1998. Photochemical transformations of surface and deep marine dissolved organic matter: effects on bacterial growth. Limnol. Oceanogr. 43 (6), 1373–1378.
Benner, R., Pakulski, J.D., McCarthy, M., Hedges, J.I., Hatcher, P.G., 1992. Bulk chemical characteristics of dissolved organic matter in the ocean. Science 255 (5051), 1561–1564.
Breitmeier, E., Voelter, W., 1989. Carbon-13 NMR Spectroscopy. Wiley-VCH.
Calza, P., Vione, D., Novelli, A., Pelizzetti, E., Minero, C., 2012. The role of nitrite and nitrate ions as photosensitizers in the phototransformation of phenolic compounds in seawater. Sci. Total Environ. 439, 67–75.
Carlson, C.A., 2002. Production and removal processes. In: Hansell, D.A., Carlson, C.A. (Eds.), Biogeochemistry of Marine Dissolved Organic Matter. Academic Press, pp. 91–151.
Carlson, C.A., Ducklow, H.W., 1995. Dissolved organic carbon in the upper ocean of the central equatorial Pacific Ocean, 1992: daily and finescale vertical variations. Deep-Sea Res. II Top. Stud. Oceanogr. 42 (2–3), 639–656.
Clarkson, C., Sibum, M., Mensen, R., Jaroszewski, J.W., 2007. Evaluation of on-line solid-phase extraction parameters for hyphenated, high-performance liquid chromatography–solid-phase extraction–nuclear magnetic resonance applications. J. Chromatogr. A 1165 (1–2), 1–9.
Coudray, C., et al., 2003. Two polyol, low digestible carbohydrates improve the apparent absorption of magnesium but not of calcium in healthy young men. J. Nutr. 133 (1), 90–93.

Dalzell, B.J., Minor, E.C., Mopper, K.M., 2009. Photodegradation of estuarine dissolved organic matter: a multi-method assessment of DOM transformation. Org. Geochem. 40 (2), 243–257.

Dittmar, T., Koch, B., Hertkorn, N., Kattner, G., 2008. A simple and efficient method for the solid-phase extraction of dissolved organic matter (SPE-DOM) from seawater. Limnol. Oceanogr. Methods 6 (June), 230–235.

Einsiedl, F., et al., 2007. Rapid biotic molecular transformation of fulvic acids in a karst aquifer. Geochim. Cosmochim. Acta 71 (22), 5474–5482.

Flerus, R., et al., 2012. A molecular perspective on the ageing of marine dissolved organic matter. Biogeosciences 9 (6), 1935–1955.

Gonsior, M., et al., 2008. Spectral characterization of chromophoric dissolved organic matter (CDOM) in a fjord (Doubtful Sound, New Zealand). Aquat. Sci. 70, 397–409 (Copyright (C) 2011 American Chemical Society (ACS). All Rights Reserved.).

Gonsior, M., et al., 2009. Photochemically induced changes in dissolved organic matter identified by ultrahigh resolution Fourier transform ion cyclotron resonance mass spectrometry. Environ. Sci. Technol. 43, 698–703.

Gonsior, M., et al., 2011. Characterization of dissolved organic matter across the Subtropical Convergence off the South Island, New Zealand. Mar. Chem. 123 (1–4), 99–110.

Gruber, D.F., Simjouw, J.P., Seitzinger, S.P., Taghon, G.L., 2006. Dynamics and characterization of refractory dissolved organic matter produced by a pure bacterial culture in an experimental predator–prey system. Appl. Environ. Microbiol. 72 (6), 4184–4191.

Gurtler, B.K., et al., 2008. Combining reverse osmosis and pulsed electrical current electro-dialysis for improved recovery of dissolved organic matter from seawater. J. Membr. Sci. 323 (2), 328–336.

Hansell, D.A., Carlson, C.A., 1998. Deep-ocean gradients in the concentration of dissolved organic carbon. Nature 395 (6699), 263–266.

Hansell, D.A., Carlson, C.A., Repeta, D.J., Schlitzer, R., 2009. Dissolved organic matter in the ocean: a controversy stimulates new insights. Oceanography 22 (4), 202–211.

Hansell, D.A., Carlson, C.A., Schlitzer, R., 2012. Net removal of major marine dissolved organic carbon fractions in the subsurface ocean. Global Biogeochem. Cycles 26 (1), GB1016.

Hertkorn, N., et al., 2006. Characterization of a major refractory component of marine dissolved organic matter. Geochim. Cosmochim. Acta 70 (12), 2990–3010.

Hertkorn, N., et al., 2007. High-precision frequency measurements: indispensable tools at the core of the molecular-level analysis of complex systems. Anal. Bioanal. Chem. 389 (5), 1311–1327.

Hertkorn, N., et al., 2008. Natural organic matter and the event horizon of mass spectrometry. Anal. Chem. 80 (23), 8908–8919.

Hertkorn, N., Harir, M., Koch, B.P., Michalke, B., Schmitt-Kopplin, P., 2013. High-field NMR spectroscopy and FTICR mass spectrometry: powerful discovery tools for the molecular level characterization of marine dissolved organic matter. Biogeosciences 10 (3), 1583–1624.

Iwamoto, K., Shiraiwa, Y., 2005. Salt-regulated mannitol metabolism in algae. Mar. Biotechnol. 7 (5), 407–415.

Kieber, D.J., McDaniel, J., Mopper, K., 1989. Photochemical source of biological substrates in sea water: implications for carbon cycling. Nature 341 (6243), 637–639.

Kim, S., Kramer, R.W., Hatcher, P.G., 2003. Graphical method for analysis of ultrahigh-resolution broadband mass spectra of natural organic matter, the Van Krevelen diagram. Anal. Chem. 75 (20), 5336–5344.

Koch, B.P., Dittmar, T., 2006. From mass to structure: an aromaticity index for high-resolution mass data of natural organic matter. Rapid Commun. Mass Spectrom. 20 (5), 926–932.

Koch, B.P., Dittmar, T., Witt, M., Kattner, G., 2007. Fundamentals of molecular formula assignment to ultrahigh resolution mass data of natural organic matter. Anal. Chem. 79 (4), 1758–1763.

Krahulec, S., Armao, G.C., Bubner, P., Klimacek, M., Nidetzky, B., 2009. Polyol-specific long-chain dehydrogenases/reductases of mannitol metabolism in *Aspergillus fumigatus*: biochemical characterization and pH studies of mannitol 2-dehydrogenase and mannitol-1-phosphate 5-dehydrogenase. Chem. Biol. Interact. 178 (1–3), 274–282.

Livesey, G., 1992. The energy values of dietary fibre and sugar alcohols for man. Nutr. Res. Rev. 5, 61–84.

Livesey, G., 2003. Health potential of polyols as sugar replacers, with emphasis on low glycaemic properties. Nutr. Res. Rev. 16, 163–191.

Loh, A.N., Bauer, J.E., Druffel, E.R.M., 2004. Variable ageing and storage of dissolved organic components in the open ocean. Nature 430 (7002), 877–881.

Mopper, K., et al., 1991. Photochemical degradation of dissolved organic carbon and its impact on the oceanic carbon cycle. Nature 353 (6339), 60–62.

Ogawa, H., Amagai, Y., Koike, I., Kaiser, K., Benner, R., 2001. Production of refractory dissolved organic matter by bacteria. Science 292 (5518), 917–920.

Pretsch, E., Buehlmann, P., Badertscher, M., 2009. Structure Determination of Organic Compounds. Springer, Heidelberg.

Repeta, D.J., Aluwihare, L.I., 2006. Radiocarbon analysis of neutral sugars in high-molecular-weight dissolved organic carbon: implications for organic carbon cycling. Limnol. Oceanogr. 51 (2), 1045–1053.

Schmitt-Kopplin, P., Hertkorn, N., Schulten, H.-R., Kettrup, A., 1998. Structural changes in a dissolved soil humic acid during photochemical degradation processes under O_2 and N_2 atmosphere. Environ. Sci. Technol. 32 (17), 2531–2541.

Schuchmann, M.N., von Sonntag, C., 1977. Radiation chemistry of carbohydrates. Part 14. Hydroxyl radical induced oxidation of D-glucose in oxygenated aqueous solution. J. Chem. Soc. Perkin Trans. 2 (14), 1958–1963.

Shakeri Yekta, S., Gonsior, M., Schmitt-Kopplin, P., Svensson, B.H., 2012. Characterization of dissolved organic matter in full scale continuous stirred tank biogas reactors using ultrahigh resolution mass spectrometry: a qualitative overview. Environ. Sci. Technol. 46 (22), 12711–12719.

Shank, G.C., Zepp, R.G., Vähätalo, A., Lee, R., Bartels, E., 2010. Photobleaching kinetics of chromophoric dissolved organic matter derived from mangrove leaf litter and floating *Sargassum* colonies. Mar. Chem. 119 (1–4), 162–171.

Sleighter, R.L., Hatcher, P.G., 2008. Molecular characterization of dissolved organic matter (DOM) along a river to ocean transect of the lower Chesapeake Bay by ultrahigh resolution electrospray ionization Fourier transform ion cyclotron resonance mass spectrometry. Mar. Chem. 110 (3–4), 140–152.

Stenson, A.C., Marshall, A.G., Cooper, W.T., 2003. Exact masses and chemical formulas of individual Suwannee River fulvic acids from ultrahigh resolution electrospray ionization Fourier transform ion cyclotron resonance mass spectra. Anal. Chem. 75 (6), 1275–1284.

Stubbins, A., et al., 2006. Open-ocean carbon monoxide photoproduction. Deep-Sea Res. II 53 (14–16), 1695–1705.

Stubbins, A., et al., 2010. Illuminated darkness: molecular signatures of Congo River dissolved organic matter and its photochemical alteration as revealed by ultrahigh precision mass spectrometry. Limnol. Oceanogr. 55, 1467–1477.

Stubbins, A., Niggemann, J., Dittmar, T., 2012. Photo-lability of deep ocean dissolved black carbon. Biogeosci. Discuss. 9 (1), 485–505.

Wang, W., Zafiriou, O.C., Chan, I.-Y., Zepp, R.G., Blough, N.V., 2007. Production of hydrated electrons from photoionization of dissolved organic matter in natural waters. Environ. Sci. Technol. 41 (5), 1601–1607.

Wang, W., Johnson, C.G., Takeda, K., Zafiriou, O.C., 2009. Measuring the photochemical production of carbon dioxide from marine dissolved organic matter by pool isotope exchange. Environ. Sci. Technol. 43 (22), 8604–8609.

Yamashita, Y., Tanoue, E., 2008. Production of bio-refractory fluorescent dissolved organic matter in the ocean interior. Nat. Geosci. 1, 579–582 (Copyright (C) 2011 American Chemical Society (ACS). All Rights Reserved.).

Zafiriou Oliver, C., True Mary, B., Hayon, E., 1987. Consequences of OH radical reaction in sea water: formation and decay of Br_2^- ion radical, photochemistry of environmental aquatic systems. ACS Symposium Series. Am. Chem. Soc. pp. 89–105.

Zafiriou, O.C., True, M.B., 1979. Nitrate photolysis in seawater by sunlight. Mar. Chem. 8 (1), 33–42.

Zafiriou, O.C., Andrews, S.S., Wang, W., 2003. Concordant estimates of oceanic carbon monoxide source and sink processes in the Pacific yield a balanced global "blue-water" CO budget. Glob. Biogeochem. Cycles 17 (1).

Zafiriou, O.C., Xie, H., Nelson, N.B., Najjar, R.G., Wang, W., 2008. Diel carbon monoxide cycling in the upper Sargasso Sea near Bermuda at the onset of spring and in midsummer. Limnol. Oceanogr. 53, 835–850 (Copyright (C) 2011 American Chemical Society (ACS). All Rights Reserved.).

Zepp, R.G., Hoigne, J., Bader, H., 1987. Nitrate-induced photooxidation of trace organic chemicals in water. Environ. Sci. Technol. 21 (5), 443–450.

Zepp, R.G., Sheldon, W.M., Moran, M.A., 2004. Dissolved organic fluorophores in southeastern US coastal waters: correction method for eliminating Rayleigh and Raman scattering peaks in excitation–emission matrices. Mar. Chem. 89 (1–4), 15–36.